Scientific Research Publishing

International Journal of Geosciences, 2026, 17(7), 478-503
https://www.scirp.org/journal/ijg
ISSN Online: 2156-8367
ISSN Print: 2156-8359

Lithological and Structural Control of the Gold Mineralization of the Souwa Prospect (Doropo), Northeastern Côte d'Ivoire

Fossou Jean-Luc Hervé Kouadio*, Ohouo Rebecca Mondah, Alain Nicaise Kouamelan, Ayo Richmond Beugré, Pierrick Courderc, Bi Fidèle Kakou

Université Félix Houphouët-Boigny Abidjan-Cocody, Laboratoire de géologie, Ressources Minérales et Energétiques (LGRME), UFR STRM, Abidjan, Côte d'Ivoire
Email: *fossou.kouadio95@ufhb.edu.ci

How to cite this paper: Kouadio, F.J.-L.H., Mondah, O.R., Kouamelan, A.N., Beugré, A.R., Couderc, P. and Kakou, B.F. (2026) Lithological and Structural Control of the Gold Mineralization of the Souwa Prospect (Doropo), Northeastern Côte d'Ivoire. *International Journal of Geosciences*, **17**, 478-503.
https://doi.org/10.4236/ijg.2026.177023

Received: June 8, 2026
Accepted: July 21, 2026
Published: July 24, 2026

Abstract

Birimian rocks host a wide range of mineralizations, of which gold is a major metal. These mineralizations are sometimes described as disseminated systems related to the circulation of mineralizing fluids in fractures generating quartz veins and veinlets, and sometimes as strongly controlled by structures (shear zones, intrusions, associated veins). These discrepancies highlight the need for detailed studies in still poorly documented areas, such as the Souwa prospect, located in the Birimian formations at the northeastern end of Côte d'Ivoire, in the Doropo department. This study aims to identify the main factors responsible for the gold mineralization at Souwa. For this purpose, macro- and microscopic petrographic analysis allowed characterization of the main lithological units, while a structural study, based on interpretation of geophysical data and examination of drill cores, identified the deformation structures and tectonics affecting the study area. Finally, the relationship between gold mineralization, host formations, and structures was established using gold grades, to better constrain lithostructural controls and guide future exploration work. The results show that the study area is dominated by granodioritic granitoids, crosscut by late dolerite dykes, affected by widespread greenschist facies metamorphism and intense hydrothermal alteration marked by sericite, silica, chlorite, epidote, and carbonate addition, as well as quartz, calcite, hematite, epidote, and ± sulfide veins and veinlets. Structurally, the Souwa prospect records polyphase ductile-brittle deformation, generating several generations of structures (quartz veins and veinlets, joints, fractures, shear zones) mainly oriented NNE-SSW, NE-SW, NW-SE, N-S, and E-W, with a predominance of NE and NW structures; these fracture networks constitute preferred pathways for the circulation and accumulation of mineralizing fluids. Gold mineralization is locally observed within the granodiorite, reflecting lithological control, and the highest grades are associated with lenses, veinlets, stockworks, and more or less brecciated quartz veins; located in intensely fractured and highly altered zones. The Souwa gold mineralization is thus interpreted as a hydrothermal mineralization controlled by both lithology and tectonics.

Keywords

Petrography, Structural, Granitoid, Gold Mineralization, Birimian, Doropo, Côte d'Ivoire

1. Introduction

The West African Craton (WAC) hosts numerous gold deposits and occurrences, mainly hosted in Paleoproterozoic Birimian formations. These formations are classically described as an alternation of granitic "ridges" and volcano-sedimentary troughs, or greenstone belts [1]. However, the stratigraphy of the Birimian has been the subject of much controversy. Based on the work of pioneers in Ghana, several authors have proposed a subdivision into a Lower Birimian, dominated by sedimentary series, and an Upper Birimian, mainly volcanic [2]-[4]. This two-"stage" scheme (B1/B2) was later extended to the entire Baoulé-Mossi domain. Other studies, in contrast, suggest an inverted succession, with a more volcanic Lower Birimian and a sediment-dominated Upper Birimian [5] [6]. In Côte d'Ivoire, [7] proposed a more integrated view, in which the "Lower" and "Upper" Birimian correspond to a largely contemporaneous sequence, where sedimentary series represent the distal facies of volcanic belts. Subsequent studies in structural mapping, geochronology, and geochemistry have reinforced this interpretation of largely co-evolutionary volcano-sedimentary belts and sedimentary basins within a Paleoproterozoic accretionary orogen [8]-[11]. These volcano-sedimentary troughs are frequently intruded by granitoids of various compositions [9]. It appears that this assemblage of Birimian rocks hosts a wide range of mineralizations, among which gold occupies a major place. According to [4] [12], the largest gold stocks are contained in the sedimentary assemblage (B1), followed by Tarkwaian conglomerates, and then the volcanic formations of the B2 assemblage. Granitoids contain only a minor fraction of the gold stock. Most deposits in West African terrains are today interpreted as late- to post-orogenic orogenic gold deposits, structurally controlled and often associated with regional shear zones and fault networks [4] [13]-[15]. However, debates persist regarding the respective roles of (i) host rocks (turbidites, mafic volcanics, conglomerates), (ii) syn- to late-tectonic intrusions, and (iii) remobilized paleo-placers in building the Birimian gold stock at the craton scale. In the Batié project, and more specifically in the Napelapera area, located in southwestern Burkina Faso, immediately north of the study area (border with Côte d'Ivoire), wide and coherent gold-mineralized zones have been identified over nearly 4 km. These zones remain open to the south, near the Ivorian border. The southern extension of the formations hosting the Batié mineralization thus arouses renewed interest in Côte d'Ivoire. One of the main obstacles to mineral exploration in this area is the lack of detailed geological data (petrography, structural architecture, metamorphic conditions, metallogenic context). Moreover, the factors controlling the emplacement and localization of gold mineralization are not yet clearly constrained. Some studies describe these mineralizations as disseminated systems related to the circulation of mineralizing fluids through fractures, generating quartz veins and veinlets, while others emphasize a predominant structural control involving shear zones, intrusions, and associated veins [13] [16]-[18]. These divergent views reinforce the need for detailed studies in still poorly documented areas on the Burkina Faso-Côte d'Ivoire border. The present study aims to contribute to elucidating these questions and improving understanding of gold mineralization in this part of Côte d'Ivoire. It is based on: (i) petrographic analysis to describe, at macro- and microscopic scales, the main rock formations encountered; (ii) structural analysis from interpretation of geophysical data and study of drill cores; and (iii) establishing the relationship between gold mineralization, host geological formations, and deformation, to better constrain the lithostructural controls of the mineralization and guide future exploration work.

2. Geological Context

2.1. West African Geology and Birimian Terranes

The West African Craton (WAC) is one of the major stable continental blocks of Africa. It covers several million square kilometers and extends from Liberia and Sierra Leone to Niger and Mauritania. Within this vast area, two major "shields" are widely exposed: the Man (or Léo) Rise to the south and the Réguibat Rise to the north, separated by the Taoudéni sedimentary basin [1]. The area of interest lies in the southern part of the craton, at the level of the Man Rise, where an ancient Archean basement is distinguished in the west (Kénema-Man domain) and a younger Paleoproterozoic domain to the east. These two domains are separated by a large transcurrent structure, the Sassandra Fault, which marks a major tectonic boundary and plays an important role in the regional architecture. East of this fault extend the Paleoproterozoic Birimian terranes (2.5 - 2.0 Ga), which form the metallogenic core of West Africa. They consist of greenstone belts (mafic to intermediate volcanics, volcaniclastics) and detrital sedimentary series (conglomerates, sandstones, pelites, quartz schists), intercalated with or bordered by vast granito-gneissic complexes of the tonalite-trondhjemite-granodiorite (TTG) type, followed by later calc-alkaline and potassic granites [6] [19] [20]. The whole was structured by the Eburnean orogeny, between about 2.2 and 2.0 Ga, which generated a succession of ductile and brittle deformation phases, the development of folded belts, regional shear zones, and regional metamorphism of variable intensity. These structures, often reactivated, today constitute the main guides for fluid circulation and the emplacement of orogenic gold deposits. In northeastern Côte d'Ivoire, this Birimian domain connects directly to the gold belts of southern Burkina Faso (notably the Boromo belt) and the Lawra belt in Ghana. Recent work shows that the granitoids of this region (Nassian in Côte d'Ivoire, Bole-Boulenga in Ghana, granitoid domains of southern Burkina) belong to the same magmatic province, emplaced in several episodes (deformed TTGs, granodiorites and potassic granites, mafic intrusions) [21]-[23]. It is within this continuous regional context, lithologically and structurally coherent, that the Souwa area on the Côte d'Ivoire-Burkina Faso border is situated.

2.2. Local Geology: Northeastern Côte d'Ivoire

The study area is located in the far northeast of Côte d'Ivoire, immediately adjacent to the Burkinabè border near Kalamon, and corresponds to the Souwa sector (**Figure 1**). It lies in the southern extension of the Birimian belts and granitoid domains described in southern Burkina Faso and around Téhini. The coordinates define a restricted but representative sector of this context, inserted within the Nassian granitoid domain. The first geological observations in the region date back to the work of [24], who reported the presence of gold around the Téhini granitoid intrusion and described a complex assemblage of migmatites, syntectonic granites (Baoulé type), and post-tectonic granites (Bondoukou type) intruding Birimian terranes. This work, complemented by that of [25], highlighted the existence of pre-Birimian orthogneisses forming part of the basement on which the Birimian series rest (**Figure 2**). More recent studies have refined this framework. References [26] [27] define the Nassian granitoid domain, characterized by a Paleoproterozoic granito-gneissic basement aged ~2.15 Ga, consisting of orthogneisses and intrusive granites. Locally, [28], as part of an Ivorian-German project, carried out detailed mapping in the Téhini region. They show that this area is composed of: greenstone belts (Téhini trough) comprising ultrabasic rocks (pyroxenites), mafic rocks (basalts, micro-gabbros, amphibolites, gabbros/norites), and more evolved volcanic rocks; "belt-type" granitoids (granodiorites, dacitic porphyries, quartz diorites/monzodiorites, muscovite granites, monzogranites); "basin-type" granitoids, dominated by one- or two-mica tonalites and granodiorites; a migmatitic granito-gneissic domain to the east, cut by numerous granitic plutons and felsic and mafic dykes.

All these units are systematically crosscut by dolerite dykes, felsic sills, quartz veins, aplites, and pegmatites, indicating a long history of fracturing and magmatic remobilization. On the Burkinabè side, [21]-[23] have shown that the granitoids located immediately to the north (southern Burkina, Bole-Boulenga domain in Ghana) are divided into several groups and magmatic episodes (ME1-ME4, G1-G5), ranging from deformed TTG plutons to little-deformed potassic granites. They propose a direct continuity between these domains and the Nassian domain in Côte d'Ivoire. The Souwa area lies precisely in this transition zone, where granitoids, greenstone belts, and major regional structures intersect. The more specialized work of [29] on the mafic, ultramafic, and granitoid rocks of the Téhini region helped correct and refine certain felsic facies described by [28], notably reclassifying some "granodiorites" as granites. Concurrently, [30], using airborne geophysical imagery over the Kalamon permit, highlighted three major families of lineaments (NE, NW, and E-W) and particularly intense fracturing in certain granitic domains. These results confirm that the region is structured by a multi-directional network of faults and shear zones, capable of guiding the circulation of mineralizing fluids. Metallogenically, the region has long been known for its gold potential. Reference [31] already mentioned, at the beginning of the 20th century, alluvial gold production in "Lobiland", straddling Côte d'Ivoire and Burkina Faso. The observations of [32] around Téhini, associating granitic intrusions, Birimian rocks, and gold placers, show that the region combines the typical ingredients of orogenic gold systems:

a Birimian and pre-Birimian granito-gneissic basement;

greenstone belts and volcano-sedimentary series;

successive magmatic episodes (TTG, granodiorites, potassic granites);

and a network of regional structures (faults, shear zones, fractures) acting as drains for hydrothermal fluids.

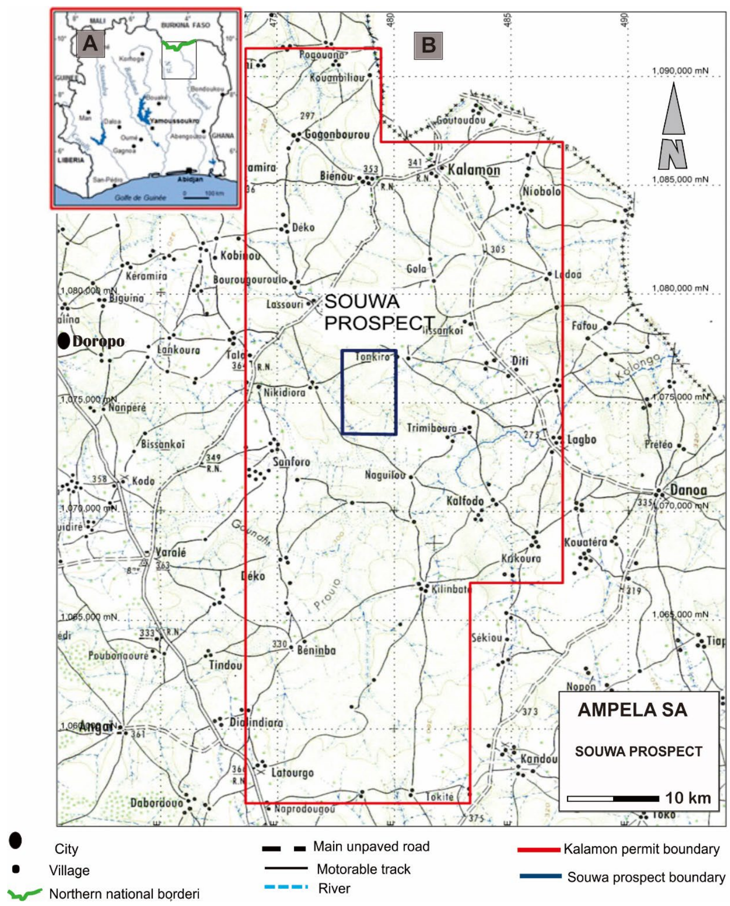

Figure 1. Maps showing the location of the Souwa prospect: (A) Map of Côte d'Ivoire showing the location of Doropo Department; (B) Doropo Department.

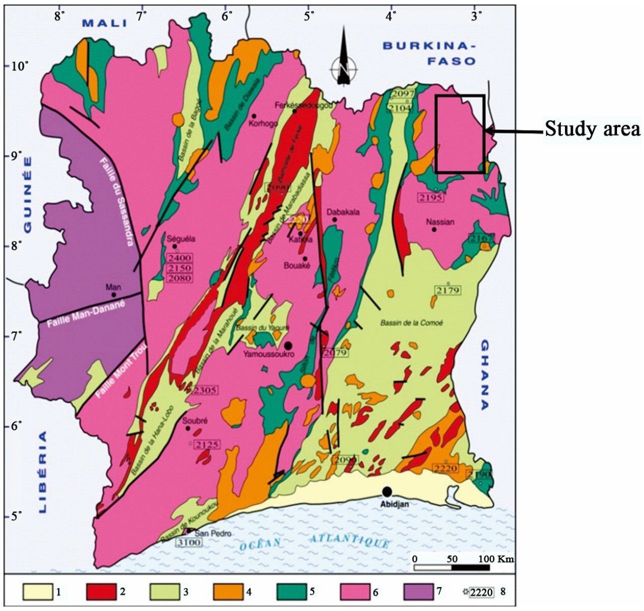

1) Archean Domain; 2) Undifferentiated granitoids and banded granites, gneisses, and migmatites (ages > 2.4 Ga); 3) Undifferentiated volcanic and volcano-sedimentary units; 4) Calc-alkaline granitoids localized within sedimentary basins; 5) Sedimentary and volcano-sedimentary basins; 6) Ferké Batholith: two-mica granitoids, locally associated with N-S striking strike-slip structures; 7) Post-Birimian formations: coastal sedimentary basin; 8) Age.

Figure 2. Simplified map of the geological domains of Côte d'Ivoire (after [6], modified). I) Archean Domain; II) Eburnean Domain; III) Transitional Domain; IV) Sedimentary Basin.

The Souwa area, located in this context of Nassian granitoids in contact with the Birimian belts of southern Burkina Faso and Téhini, thus appears as a key sector to test the relationships between:

(i) the nature of the host lithologies (granitoids, greenstones, volcano-sedimentary formations);

(ii) the structural architecture (faults, shears, fractures);

and (iii) the distribution of gold mineralization.

It is precisely this articulation between the Birimian regional framework, local basement architecture, and litho-structural controls that the present study proposes to explore at the scale of the Souwa prospect.

3. Analytical Methods

In this study, we implemented a multidisciplinary approach combining documentary compilation, drill core analysis, geophysics, structural geology, petrography, and geochemistry. An initial documentation phase (theses, articles, reports, 1/50,000 topographic and 1/200,000 geological maps) allowed us to place the area in its regional context and guide the choice of boreholes to study. Fieldwork focused exclusively on oriented cores (a total of around 50 drill holes, averaging 250 metres in depth, were studied. The total length of these holes was 12,500 metres), from which ten representative samples of the main facies (notably granodiorite and dolerite) were selected, prioritizing fresh and homogeneous rocks, while also including some altered samples to characterize hydrothermal alteration phases. The litho-structural analysis is based on airborne geophysical data (magnetism and gamma-ray spectrometry) pre-processed and interpreted by superposition with the DEM to map major lithological units and lineaments, supplemented by statistical analysis of structure orientations using rose diagrams (GéOrient, GeoRose). At the core scale, the geometry of structures (quartz veins, fractures, contacts, shear zones) was quantified by measuring α and β angles with a goniometer, then converted to azimuths and dips (GeoCalculator) to establish stereographic projections and directional families. Macroscopic petrography, performed with a hand lens on standardized sheets, allowed description of textures, mineral assemblages, sulfides, alterations, and deformation style (with dilute hydrochloric acid tests and magnetic pen), while Micromine software was used to visualize drill sections and the vertical distribution of facies. This approach was complemented by microscopic petrographic study on ten thin sections, observed under a polarizing microscope at the Basement Geology and Metallogeny Laboratory, to specify mineral assemblages, microstructures, and alteration parageneses, and to propose a consistent rock nomenclature. Core sampling was conducted at 0.80 m to 1.20 m intervals, incorporating QAQC inserts (blank, duplicate and standard). In mineralised zones, special care was taken to avoid diluting gold grades. Finally, the gold grades of the sampled cores were determined by the fire assay method at the Bureau Veritas laboratory, with a detection limit of 0.01 ppm, and then integrated into grade-depth profiles for each drill hole (Excel) to identify and characterize mineralized zones.

4. Results

4.1. Petrographic Data

Petrographic study revealed the existence of a granodiorite intrusion cut by dolerite dykes in the drilled cores (**Figure 3** and **Figure 4**).

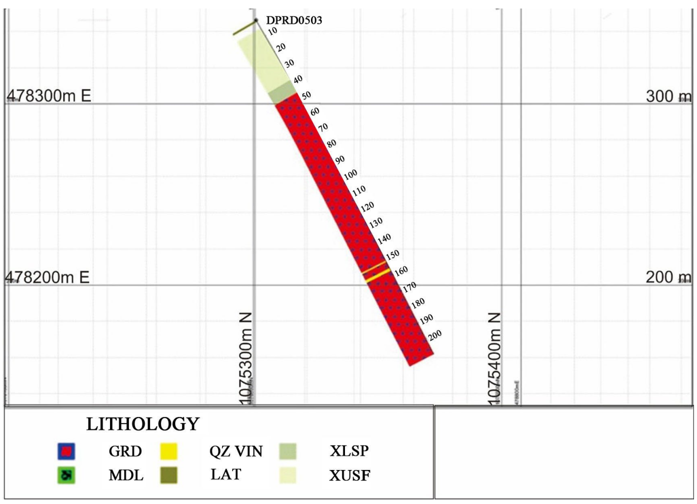

Lithological units: GRD: granodiorite; MDL: dolerite; XLSP: lower saprolite; XUSP: upper saprolite; LAT: laterite; QZ VIN: quartz vein.

Figure 3. Synthetic petrographic log of drillhole DPRD0503.

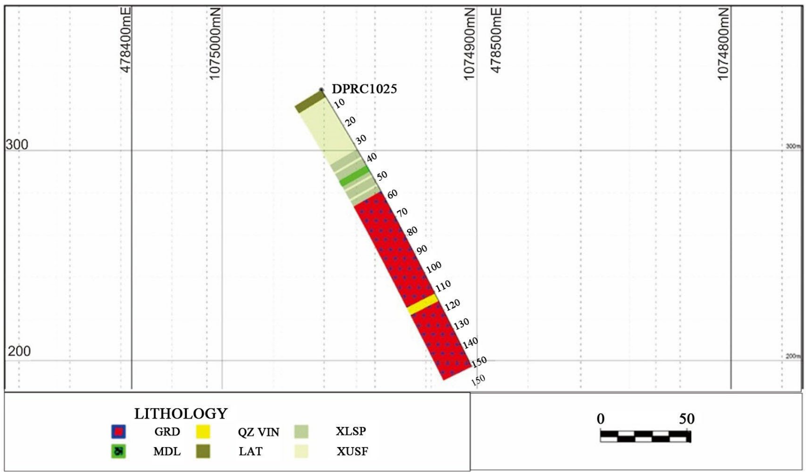

Lithological units: GRD: granodiorite; MDL: dolerite; XLSP: lower saprolite; XUSP: upper saprolite; LAT: laterite; QZ VIN: quartz vein.

Figure 4. Synthetic petrographic log of drillhole DPRC1025.

4.1.1. Granodiorites

The granodiorite constitutes the dominant lithology of the Souwa prospect. It has a granular texture, medium to coarse-grained, massive in appearance, overall mesocratic. Mineralogically, it is essentially composed of plagioclase (≈ 45% - 50%), quartz (≈ 30% - 35%), biotite (≈ 10% - 15%), green amphibole (hornblende, ≈ 10% - 12%), and alkali feldspar (orthoclase, ≈3% - 5%), with additional primary accessory minerals (sphene) and secondary minerals (chlorite, epidote, sericite, opaque minerals).

Plagioclases, euhedral to subhedral, show widely varying sizes and often altered polysynthetic twins. They frequently exhibit zoning with an altered calcic core and clear, more sodic borders, as well as large partially sericitized areas. Quartz occurs as globular crystals or xenomorphic patches, ranging in size from micro-grain to coarse grain, with distinct undulatory extinction. Ferromagnesian phases are represented by biotite and green hornblende. Biotite occurs as subhedral to euhedral lamellae, brown to light green due to partial chloritization, with direct pleochroism and spotty zircon inclusions surrounded by a dark halo. Hornblende forms medium, elongated crystals, strongly pleochroic in green, with two well-marked rhombic cleavages and frequent optical zoning. It is generally associated with biotite. Alkali feldspar (orthoclase) occurs as more or less sericitized phenocrysts or interstitial microcrystals, often twinned according to the Carlsbad law.

Primary accessory minerals are dominated by sphene (titanite), euhedral, rhombic, with high relief, sometimes slightly fractured. Secondary alteration products consist of chlorite, epidote, sericite, and opaque minerals (sulfides and oxides). Epidotes, with high relief and vivid polarization tints, develop mainly in plagioclases and amphiboles; sericite appears as fine flakes in feldspars (**Figure 5**). Opaques, xenomorphic to subhedral, with varied shapes (cubic, rectangular, subrounded), are located at the edges of accessory minerals or in partial to total replacement of ferromagnesian phases, indicating hydrothermal alteration.

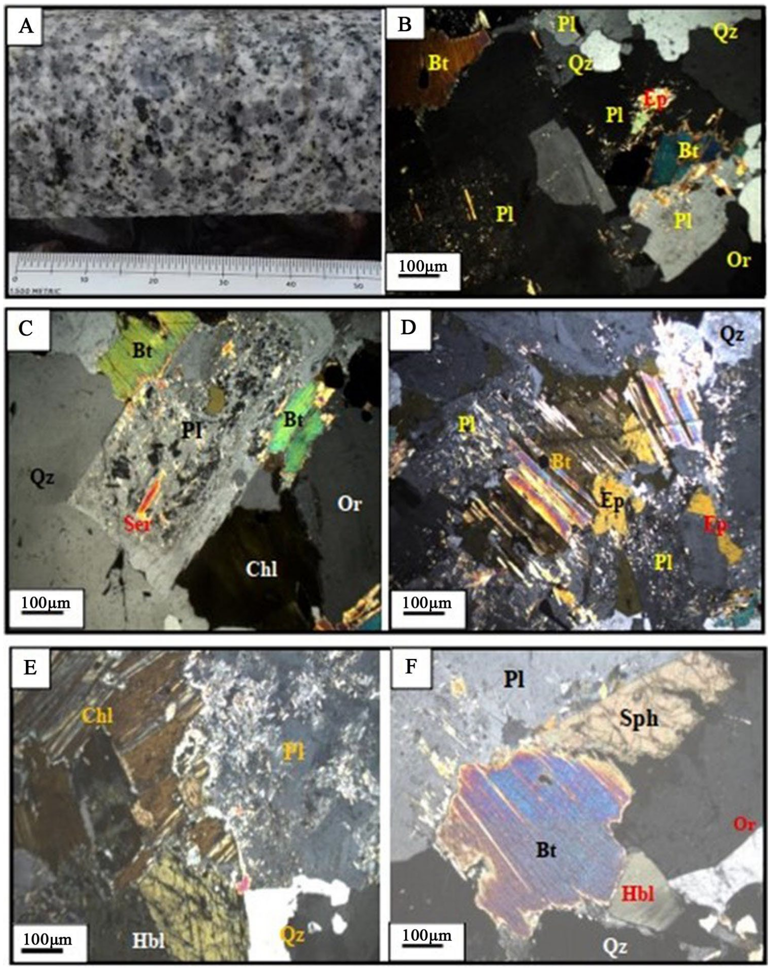

Pl: plagioclase; Qz: quartz; Or: orthoclase; Bt: biotite; Hbl: green hornblende; Ep: epidote; Ser: sericite; Chl: chlorite; Sph: sphene (titanite).

Figure 5. Macroscopic features and photomicrographs of the granodiorite: A: granodiorite core sample; B: granodiorite showing the arrangement of the different mineral phases; C: sericitization and damouritization of plagioclase; D: biotite undergoing chloritization; E: zoned amphibole at the contact with chlorite phenoblasts; F: primary sphene associated with biotite.

4.1.2. Dolerites

The hypovolcanic rocks of the study area correspond to mafic dolerite dykes. They are melanocratic, massive in appearance, with a typical microgranular doleritic texture. Macroscopically, they consist of abundant small black pyroxene crystals and micro-grains of plagioclase visible to the naked eye (**Figure 6**).

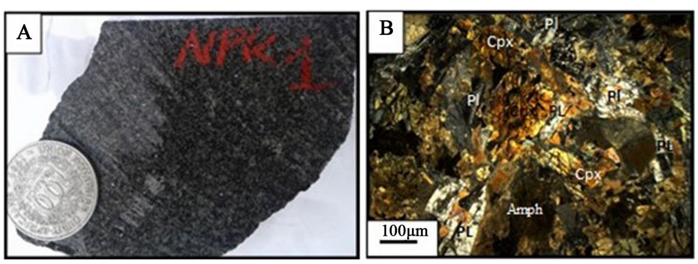

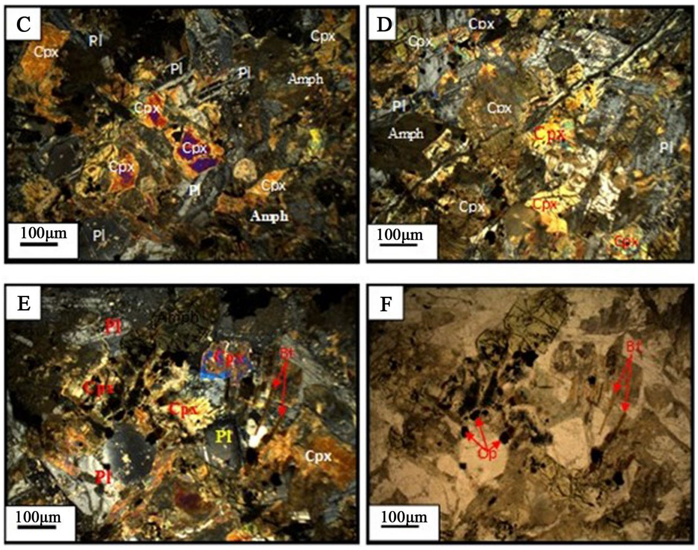

Pl: plagioclase; Cpx: clinopyroxene; Bt: biotite; Amph: amphibole; Op: opaque minerals.

Figure 6. Macroscopic and microscopic features of dolerites. A: macroscopic aspect of dolerites; B: intergrown plagioclase associated with pyroxenes; C: pyroxene destabilized into amphibole; D: pyroxene-plagioclase-amphibole paragenesis; E & F: paragenesis associated with biotite and opaque minerals.

Under the microscope, the normal doleritic texture shows a pyroxene-plagioclase association. Pyroxenes (≈40% - 50%), the major phase, are essentially clinopyroxenes (augite) in stubby to sub-rounded prisms, with medium to high relief. They exhibit fine, regular cleavage in longitudinal section and two sub-orthogonal cleavages in cross-section, with an extinction angle of about 38˚. Augite is frequently surrounded by an amphibole halo (actinolite) related to uralitization, sometimes resulting in a brighter central zone and less bright borders.

Plagioclases (≈40% - 45%) form numerous interwoven laths of medium to coarse size, mostly showing polysynthetic twins. They exhibit incipient saussuritization materialized by the appearance of epidote and sericite.

Biotite is represented only by rare crystals as fine laths (≈1%), subhedral.

Accessory minerals are essentially secondary and belong to the alteration paragenesis (actinolite, epidote, oxides, and rare opaques), products of saussuritization of plagioclases and uralitization of pyroxenes. Augite is thus partially or totally transformed into actinolite, the neomorphic amphibole generally preserving the crystal orientation of the original pyroxene.

4.2. Alteration

The lithological study shows that the Souwa formations have undergone two main types of processes: superficial meteoric alteration, generating regolith thicknesses on the order of 40 to 70 m and deeper hydrothermal alteration, closely linked to mineralization.

Analysis of the transformations of primary minerals in the granodiorite allows distinction of two modes of hydrothermal alteration (**Figure 7A** and **Figure 7B**;

Figures 8-9):

(1) pervasive alteration, and (2) vein-type alteration.

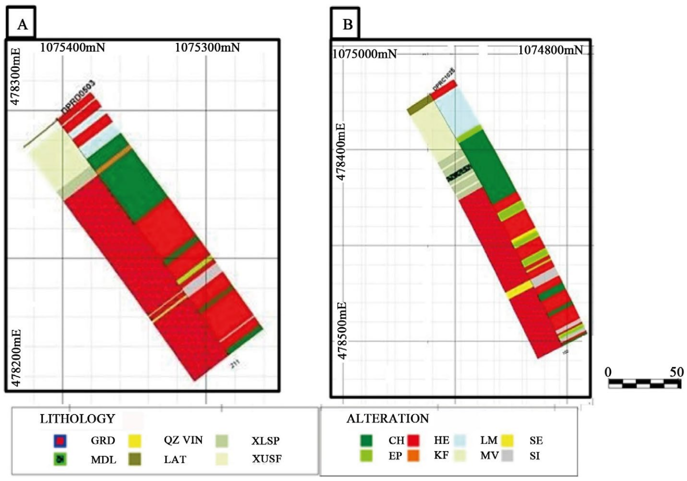

GRD: granodiorite; MDL: dolerite; XLSP: lower saprolite; XUSP: upper saprolite; LAT: Laterite; QZ VIN: quartz vein. CH: chlorite; HE: hematite; LM: limonite; SE: sericite; EP: epidote; KF: potassium feldspar; MV: muscovite; SI: silica.

Figure 7. Log of distribution of alteration minerals along drillholes; A) drillhole DPRD 0503; B) drillhole DPRC 1025.

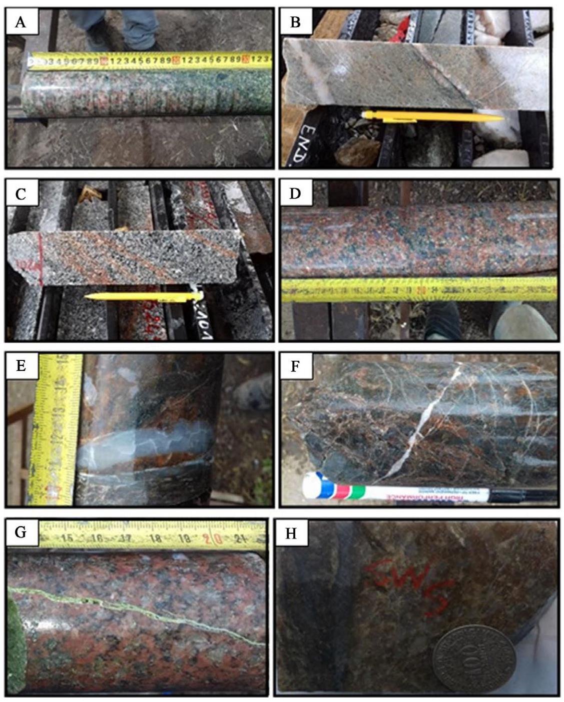

Figure 8. Macroscopic features of pervasive and vein-type alteration phases: A: pervasive alteration in chlorite, epidote, and hematite; B: sericitized granodiorite crosscut by quartz-calcite veinlets; C: unaltered granodiorite crosscut by hematite veinlets; D: pervasive alteration in hematite and chlorite; E & F: altered granodiorite crosscut respectively by sericitized quartz and calcite veinlets; G: epidote-filled joint (fluor green) in hematized granodiorite; H: smoky quartz veinlets in sericitized granodiorite.

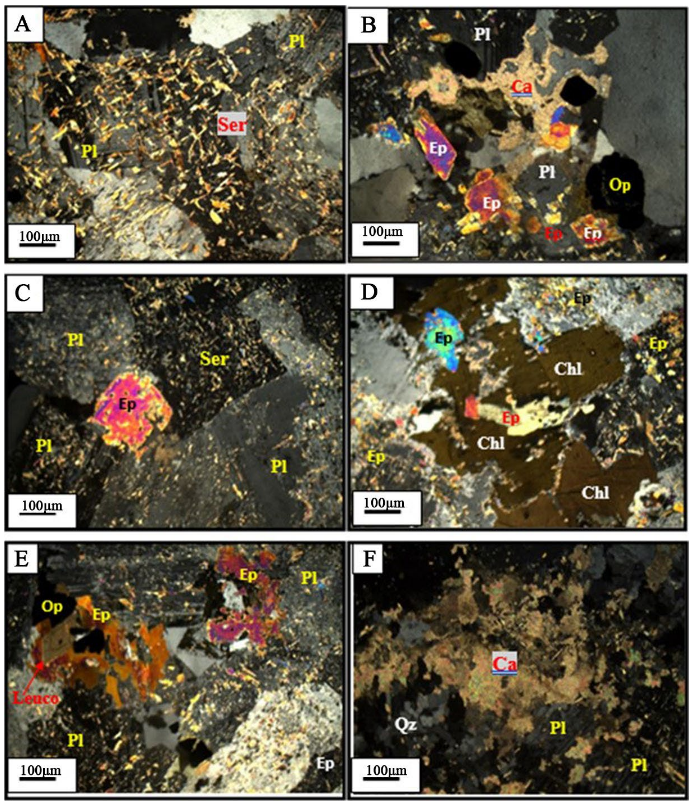

Figure 9. Microscopic features of pervasive alteration phases: A: sericite developed at the expense of plagioclase; B: transformation of plagioclase into epidote and calcite; C: plagioclase phase exhibiting saussuritization, sericitization, and albitization; D: chlorite aggregates associated with epidote; E: assemblage of epidote, leucoxene, and opaque minerals; F: calcitization of plagioclase and amphiboles.

The pervasive and vein-type alterations at the Souwa prospect reflect intense hydrothermalism, closely related to the circulation of mineralizing fluids within the granodiorite and dolerite dykes.

Pervasive alteration affects the entire rock and is manifested by the replacement of primary minerals (feldspars, biotites, amphiboles) by a secondary paragenesis, accompanied by general discoloration (Figure 8A-C); the main processes identified are sericitization, epidotization, chloritization, carbonation, silicification, hematitization, and sulfidation. As the dominant process, sericitization as shown in Figure 8H corresponds to the destabilization of plagioclases and biotites, replaced by fine flakes of white micas (a few tens of microns), with plagioclases showing marked "clouding" and heterogeneous distribution of sericite linked to their original zoning (Figure 9A and Figure 9B).

Epidotization mainly affects plagioclases and amphiboles, in the form of epidote grains dispersed in these phases (Figure 9B-E), macroscopically appearing as pistachio-green crystals (pistacite; Figure 8A) and showing vivid polarization tints from yellow-orange (zoisite) to bluish-green (clinozoisite), often associated with small sulfides, sphene (leucoxene), and quartz. Chloritization reflects the transformation of ferromagnesian minerals (biotite, amphibole), partially to totally, into greenish chlorite lamellae with pleochroism colorless to pale green, clear cleavages, and low birefringence (**Figure 9D**), giving the rock a dark green tint (**Figure 8A**). Carbonation manifests mainly by calcitization of plagioclases and amphiboles, in the form of iridescent calcite patches, often associated with sericite and organized into polycrystalline aggregates within crystals or along intragranular microfractures (**Figure 9B** and **Figure 9F**; **Figure 10A**). Silicification corresponds to an impregnation of the host rocks by small additional quartz crystals with interlocking and often oval outlines (**Figure 11B**), indicating early crystallization from fluids very rich in SiO_2. Hematitization mainly affects the granodiorite, giving it a reddish color; in thin section, hematite appears as opaque minerals (**Figure 8D-F**) resulting from the partial or total replacement of ferromagnesian minerals and sulfides. Sulfidation, finally, corresponds to the formation of sulfides, mainly cubic pyrite, more marked in highly deformed and altered zones, where pyrite grains, opaque in transmitted light (**Figure 10B** and **Figure 10C**), are either disseminated in the host rocks or concentrated in tectonoclasts within veins.

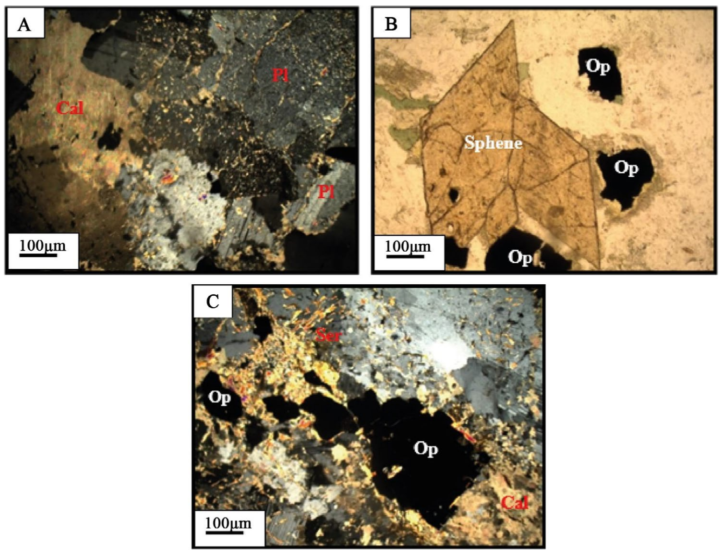

A: calcitization of plagioclase and amphiboles; B: titanite (sphene) associated with opaque minerals; C: opaque minerals resulting from the destabilization of ferromagnesian minerals, generally associated with secondary minerals. Pl: plagioclase; Chl: chlorite; Ser: sericite; Ca: calcite; Op: opaque minerals.

Figure 10. Microscopic features of alteration phases.

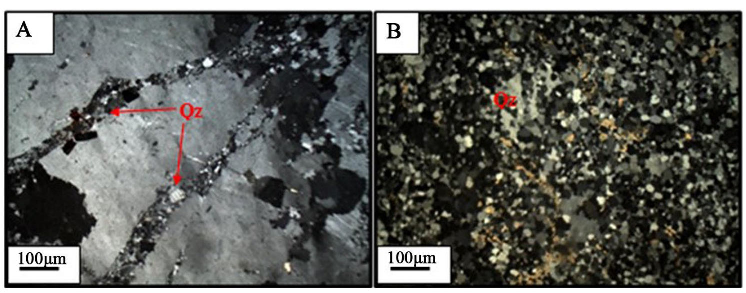

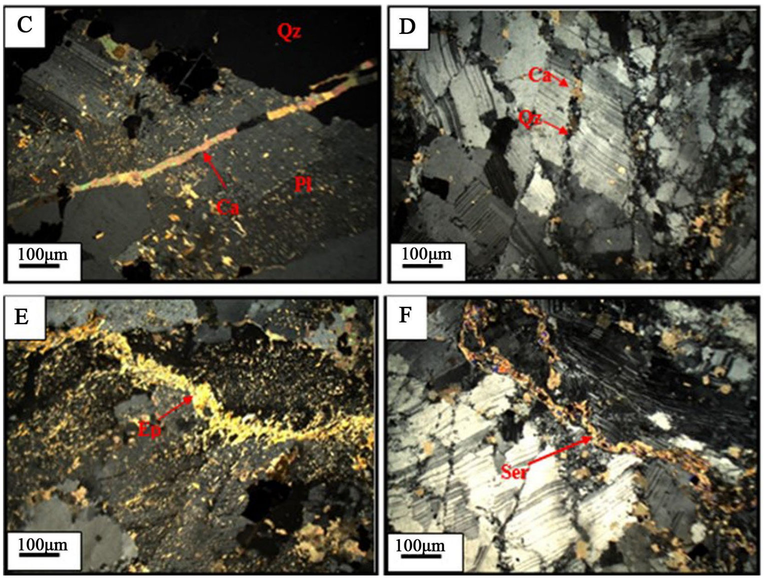

A: quartz veinlets; B: silicification marked by quartz microcrystals associated with calcite; C: calcite veinlets crosscutting plagioclase and quartz; D: microfractures filled with quartz and calcite; E: epidote in veinlets; F: sericite in veinlets associated with calcite and opaque minerals. Pl: plagioclase; Ser: sericite; Ca: calcite; Ep: epidote; Qz: quartz.

Figure 11. Microscopic features of vein and pervasive alteration phases.

Vein-type alteration is expressed by a network of veins and veinlets crosscutting the granodiorite, with varied fillings and bordered by pervasive alteration halos (Figure 8A-F; Figure 11): quartz-rich veinlets (see Figure 8H), 0.1 to 5 cm thick, highlighting silicification and resulting from the sealing of fractures by hydrothermal fluids highly enriched in silica (Figure 11A and Figure 11D); calcite veinlets, 0.1 to 1.5 cm thick, cutting indiscriminately through the rock, calcite being alone (Figure 8F; Figure 11C) or associated with quartz (Figure 8E; Figure 11D); irregular epidote-rich veinlets, consisting of yellow lamellae grouped locally into small aggregates (Figure 8G; Figure 11E); and irregular sericite-rich veinlets, marked by alignments of sericite lamellae, sometimes in aggregates associated with calcite, pyrite, and more rarely hematite grains (Figure 11F).

4.3. Lithological Mapping

The map derived from a total magnetic intensity (TMI) and a first vertical derivative of reduced to pole remote analysis (1VDRTP), Figure 12 shows distinctive characteristics (shapes, color, tint intensity, textures, contrasts, and a range of varying magnetic susceptibilities corresponding to a color set) allowing three main lithological units (I, II, and III) to be distinguished (Figure 13). This technique allows you to better define geological structures (such as faults and rock contacts) by moving the anomalies to a position above their sources. When combined with field data, these well-defined units, which are unevenly distributed throughout the region, essentially correspond to two granitoid units (I and II) and one mafic unit (III) (Figure 13).

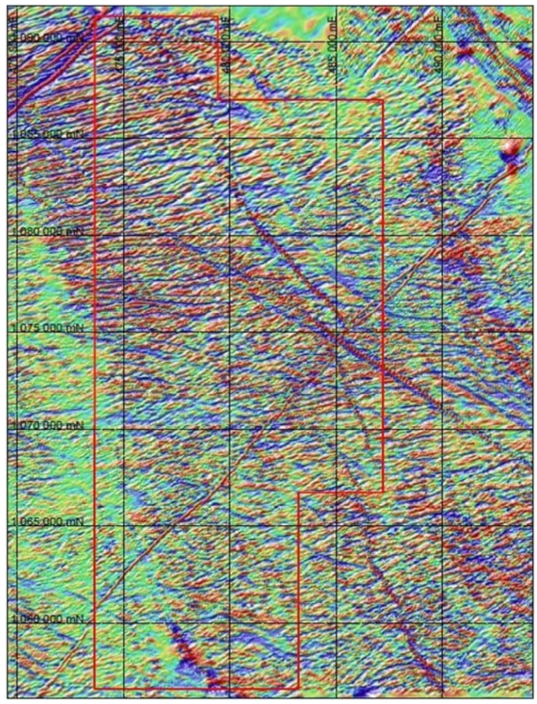

Figure 12. TMI_1VDRTP geophysical map.

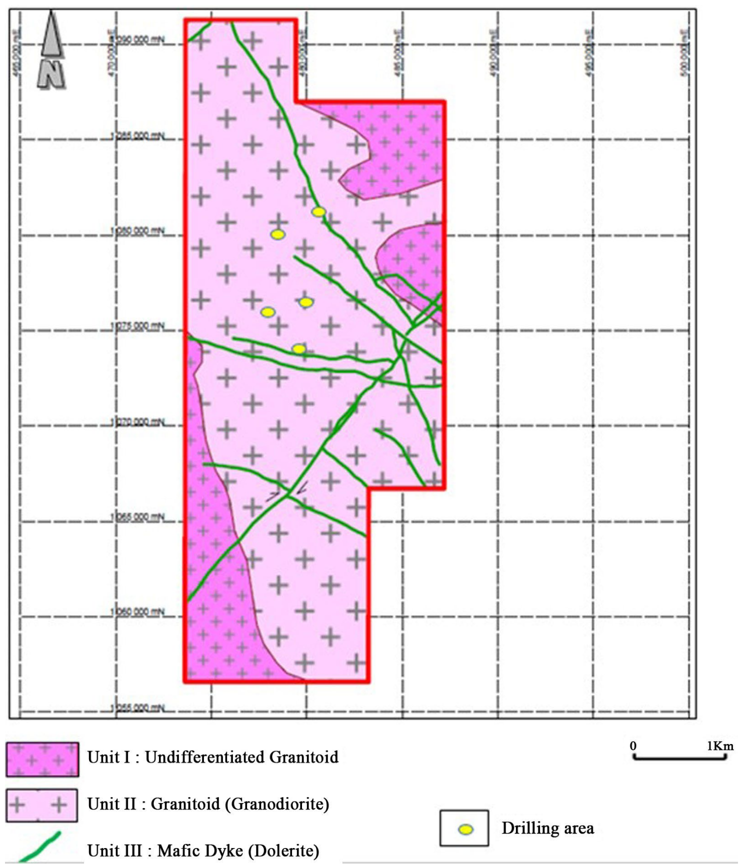

Figure 13. Preliminary lithological map of the study area derived from geophysical and field observations (after [30]).

- Unit I: This is a granitoid with a slightly rough texture, with magnetic susceptibilities between 1.89 and 3.84 10^{-3} SI and a density varying from 2.54 - 2.74 10^3 kg/m^3; it appears in a yellowish-green tone. It seems to be in sharp contact with Unit II.

- Unit II: This corresponds to the most extensive and dominant lithological unit of the Kalamon permit. This unit corresponds respectively to rough-textured granitoids, with magnetic susceptibility varying from 1.30 - 9.76 10^{-3} SI and density varying from 2.54 - 2.69 10^3 kg/m^3. It appears in a dark red-blue coloration associated with yellow tones haloed in sky blue. This rock seems to intrude Unit I. The images indicate an unusual abrupt change between Unit II and I, which undoubtedly corresponds to a lithological contact.

- Unit III: These correspond to mafic intermediate rock dykes, crosscutting the previous units, undoubtedly the most recent. Their magnetic susceptibilities vary from 2.11 - 7.18 10^{-3} SI (strong response) with a density varying from 2.56 - 2.99 10^3 kg/m^3. They appear in a red coloration.

The Souwa prospect consists essentially of Unit II. It corresponds to a granodioritic pluton which appears as the most unstable and therefore most deformed formation. Then come Units III corresponding to the dolerite dykes crosscutting Unit II. The curved boundaries, the unusual abrupt change, and the unstable character of the granodioritic pluton suggest that this granitoid is syn- to late intrusive.

4.4. Structural Analysis

Structural analyses of the Souwa prospect come from visual and manual interpretations of geophysical images (**Figures 12-14**), complemented by the study of drill cores and statistical analysis on stereograms (Géorient software), and highlight a dense network of lineaments (**Figure 14**) within the granitoids, interpreted as fractures, joints, foliations, banding, or schistosities (Ouattara, 1998). The lineaments, ranging from metric to plurikilometric in length, are distributed into three main families: NE-SW (N30˚ - N70˚), the most abundant, NW-SE (N110˚ - N130˚), and E-W (N080˚ - N100˚), defining a fracture system related to ductile-brittle deformation. On the cores, several families of mesostructures related to these tectonics are recognized: quartz veins and veinlets, fractures, joints, faults, mineral stretching lineations, and lithological contacts. Quartz veins, centimetric to metric in thickness (**Figure 15A**), and veinlets, very abundant, form a network of quartz-filled fractures, sometimes associated with calcite, chlorite, epidote, and hematite, with three dominant orientations: NW-SE dipping SW (mean plane N130, 45˚SW), NE-SW dipping NW (mean plane N40, 35˚NW), and N-S submeridional (mean plane N5, 10˚NW) (**Figure 16A**). Joints, fissures without visible displacement, sometimes lined with epidote, hematite, and chlorite (**Figure 15D**), mainly show a NNE-SSW orientation dipping NW (mean plane ~N37˚, 56˚NW), with rarer NNW-SSE directions (**Figure 16C**). Shear zones, areas of intense deformation especially in the granodiorites, are characterized by mineral stretching lineation with plunges of 40˚ to 70˚ towards the SE (**Figure 15B** and **Figure 16D**).

The observed lithological contacts mainly concern the upper and lower dolerite-granodiorite contacts and quartz vein-granodiorite contacts, with a dominant NE-SW (N38˚) direction dipping about 30˚NW, with locally NW-SE orientations (**Figure 15C** and **Figure 16E**). Fractures sensu stricto, very frequent and multi-directional (**Figure 16E**), cut through the entire rock; the main measured families are NE-SW dipping NW (mean plane N60˚, 50˚NW), N-S dipping west (54˚W), and E-W dipping NW (mean plane N280˚, 35˚NW). Overall, the region corresponds to a large granitoid zone (units I and II) rich in lineaments and cut by mafic dykes, dominated by NE and NW directions, with a significant contribution of E-W structures; the Souwa prospect, located in Unit II, the most deformed, is characterized by the predominance of brittle structures (fractures, joints, veinlets, and quartz veins) associated with ductile structures (mineral stretching lineations), the main directions being NNE-SSW, NE-SW, NW-SE, N-S, and E-W, with dips mostly oriented NW for NE-SW structures and SW for NW-SE structures, confirming the predominance of NE and NW directions revealed by geophysical data.

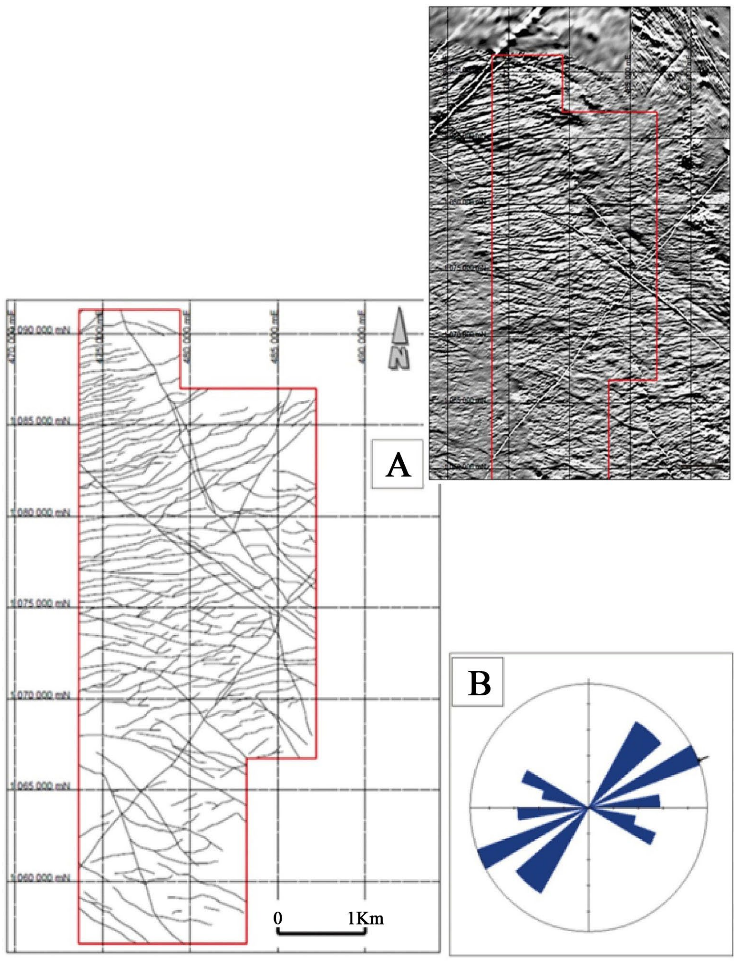

Figure 14. Image TMI_1VDRTP showing the lineaments. A) Lineament network map of the study area (after [30]) and B) directional rose diagram of mapped lineaments.

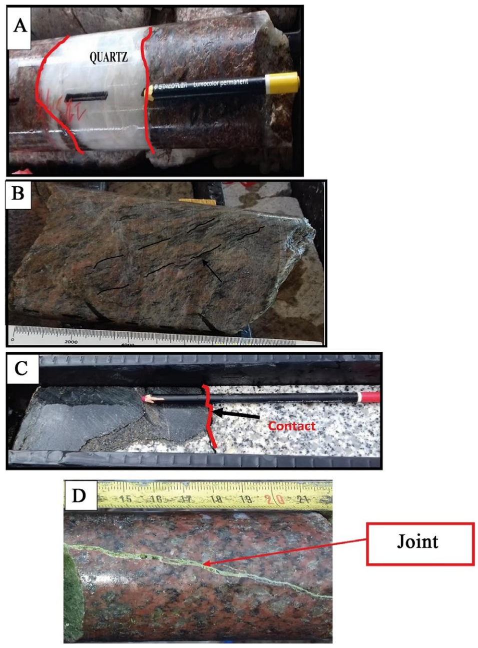

Figure 15. Macroscopic characteristics of selected mesostructures observed in drill cores from the study area: (A) strongly hematized granodiorite crosscut by a quartz vein; (B) shear zone characterized by mineral stretching; (C) contact zone between a dolerite dyke and the granodiorite; (D) joint infilled with epidote.

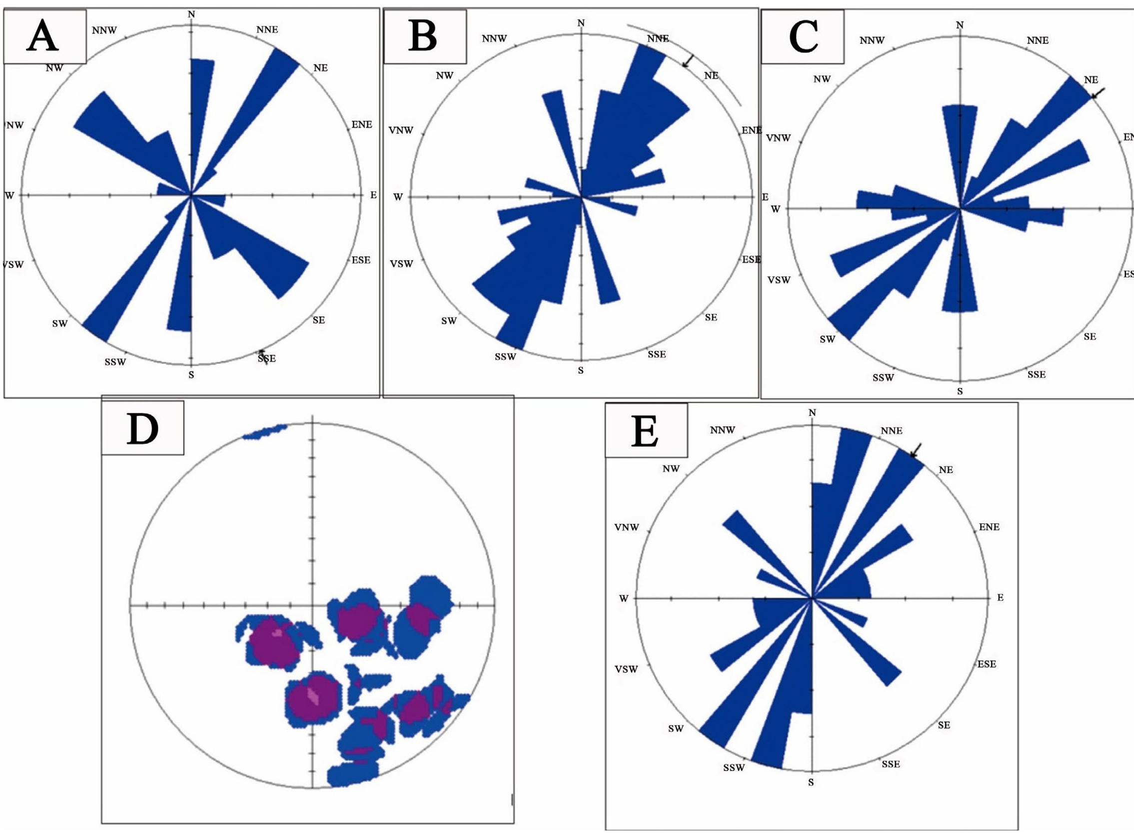

Figure 16. Rose diagrams of structural elements in the study area: (A) quartz veins and veinlets, (B) joints, (C) stretching lineation, (D) lithological contacts, and (E) fractures.

4.5. Mineralization of the Study Area

The Souwa gold mineralization is hosted in the granodiorites. These rocks have been affected by significant hydrothermal alteration marked by quartz veins and quartz-calcite veinlets. This hydrothermal alteration induced pervasive alteration of the host rocks, the most important being silicification, carbonation, sericitization, and sulfidation (**Figure 17**). Gold mineralization at Souwa was locally observed within the granodiorite. Dolerite, on the other hand is not mineralized. Thus, this gold mineralization exhibits lithological control (**Figure 17**, **Table 1**). The tectonics of the Souwa prospect is characterized by the presence of fractures, veins, veinlets, faults, joints, stretching lineations. These different structures have directions that generally follow those of the Eburnean overall (NE-SW to NNE-SSW). Quartz veins and veinlets associated with sulfides are frequent in the mineralized intervals. Drill hole intervals showing the highest gold grades are linked to quartz veins, which are located in zones with fractures, faults, and shears associated with silicification, calcitization, sericitization, and sulfidation (**Figure 18**). Thus, the mineralization of the Souwa prospect is of hydrothermal affiliation, tectonically controlled. Oxidation shows 1.2 g/t at 11 m, probably linked to sulfide quartz veinlets, and the dolerite is not mineralized. Interesting gold grades are therefore essentially obtained in the granodiorite, the dominant host rock, and the richest intervals (**Figure 17** and **Figure 18**) correspond to zones where silicification, carbonation, sulfidation, and sericitization overlap, whereas moving away from the mineralized zones, an increase in chlorite and epidote and a decrease in the quartz-carbonate-sericite-sulfide assemblage are observed; the major alterations are thus silicification, carbonation, sericitization, and sulfidation, with chloritization, epidotization, and hematitization being less developed (**Figure 17** and **Figure 18**). The deformation is ductile-brittle, and the graphs show that zones crossed by quartz veins and veinlets, whether in fresh rock or in the oxidation zone, constitute potential zones for gold mineralization. Gold, not visible to the naked eye even in the richest intervals, must be extremely fine and associated with sulfides, mainly pyrite, present in the granodiorite and in the gold-bearing quartz veins, in the form of cubes, disseminated, as aggregates, or as veinlets, with hematite also present (**Figure 18**). Two types of mineralization are distinguished: (i) a disseminated mineralization, illustrated by hole DPRC1025 at 25 and 40 m (2.30 and 2.81 g/t) with no associated quartz vein (**Figure 18**), and (ii) a vein-type mineralization, the most frequent, materialized by quartz veins, the highest grades being observed in zones crosscut by these veins (DPRC1025: 7 g/t at 100 m; DPRC10503: 4.96 g/t at 90 m; **Figure 17** and **Figure 18**). Overall, the Souwa gold mineralization, controlled both by lithology (host granodiorite altered by quartz veins and quartz-calcite veinlets, **Table 1**) and by tectonics (fractures, faults, joints, veins, veinlets, and stretching lineations with NE-SW to NNE-SSW directions characteristic of the Eburnean orogeny), is of hydrothermal type, concentrated in zones of fractures, faults, and shears associated with intense silicification, calcitization, sericitization, and sulfidation.

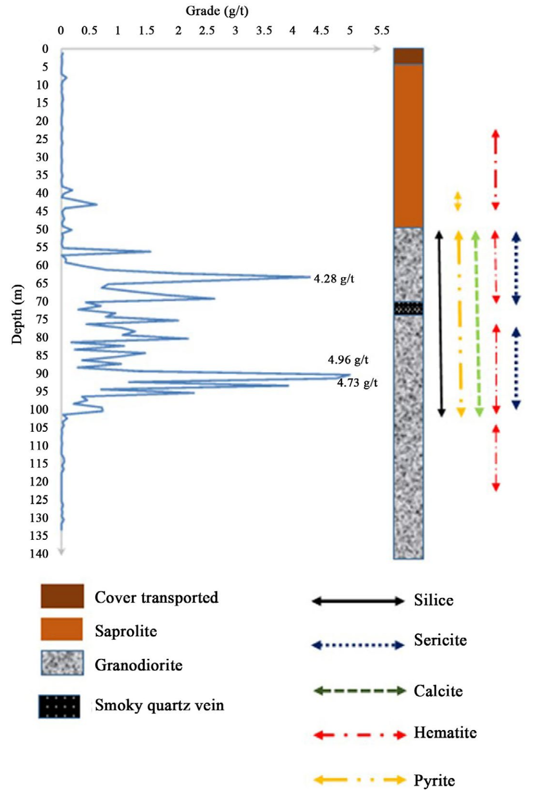

Figure 17. Gold grade (g/t) vs depth along drillhole DPRD 0503. Rocks and alterations.

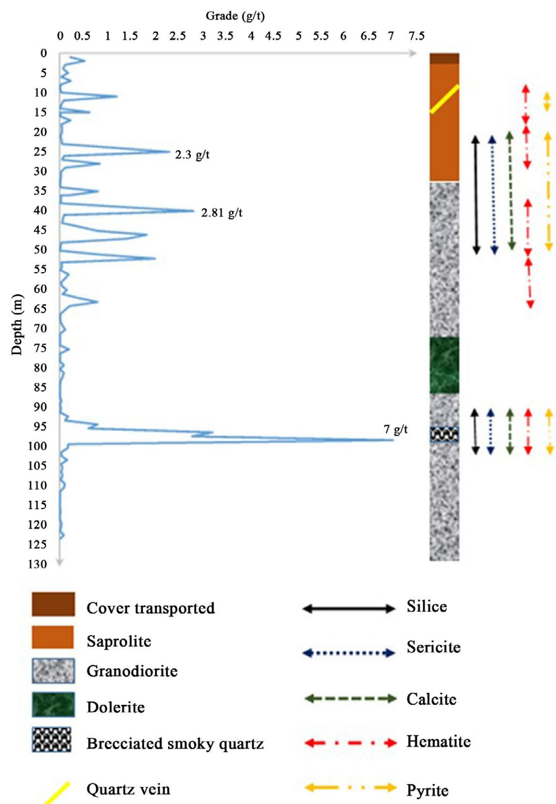

Figure 18. Gold grade (g/t) vs depth along drillhole DPRC1025. Rocks and alterations.

Table 1. Below is a list of some of the samples analysed for gold in the drill hole, DPRD003.

Drill Hole	Sample ID	Depth m	Gold grade g/t	Description
DPRD003	Sample 1	120.50 to 121.80	0.001	Dolerite
DPRD003	Sample 2	128.35 to 129.55	0.001	Unaltered granodiorite
DPRD003	Sample 3	145.14 to 146.34	0.002	Slightly altered granodiorite (epidote-chlorite-hematite)
DPRD003	Sample 4	158.20 to 159.40	1.9	Granodiorite with moderate silicification and sericitisation, cut by smoky quartz and carbonate veinlets, with disseminated pyrite
DPRD003	Sample 5	167.42 to 168.62	2.67	Hightly silicified granodiorite with moderate hematitization and abundant disseminated pyrite
DPRD003	Sample 6	168.62 to 169.82	2.80	Hightly silicified granodiorite with moderate hematitization, and abundant disseminated pyrite
DPRD003	Sample 7	179.05 to 180.05	4.80	Granodiorite with strong silicification, hematization and sericite alteration, as well as quartz-carbonate veinlets. with disseminated pyrite and leucoxene
DPRD003	Sample 8	180.05 to 181.25	5	Granodiorite with strong silicification, hematization and sericite alteration, as well as quartz-carbonate veinlets. with disseminated pyrite and leucoxene
DPRD003	Sample 9		0.002	Slightly altered granodiorite (epidote-chlorite-hematite)

5. Discussion

Lithologically, the Souwa prospect consists of a granodioritic pluton cut by dolerite dykes; the granodiorite, with a medium to coarse-grained matrix, composed of plagioclase, quartz, biotite, hornblende, orthoclase, and accessory sphene, has a composition identical to the granodiorites of the ME 2 plutonic event described in southern Burkina Faso by [21] and comparable to the G3 group defined in northwestern Ghana by [22], as well as to the "belt-type" granodiorites identified in the Téhini region by [28], while differing from the "basin-type" granodiorites of the same region in terms of mineralogical composition; all the lithologies of the prospect have been affected by a regional greenschist facies metamorphism described by [24], similar to that of many West African gold deposits [33]-[38], except for Konongo in Ghana, where metamorphism reaches a higher degree (biotite + garnet; [39]) and where [38] and [34] locally note an amphibolite facies (Tiébélé, Agbahou); the Souwa prospect is furthermore characterized by a thick meteoric alteration reaching up to 70 m, superimposed on intense hydrothermal alteration, both pervasive and vein-type, marked by sericitization, carbonation, silicification, epidotization, chloritization, sulfidation, and hematitization, analogous to the assemblages described at Bonikro [36], [35] and Agbahou [34]. Structurally, the area records ductile-brittle deformation expressed by NE-SW, NW-SE, N-S to NNE-SSW, and E-W structures. The measurements taken in the field agree with the directions of lineaments and corroborate the major directional classes defined on the Kalamon permit [30], as in Téhini [28], where several generations of quartz veins and veinlets, with a general NNE-SSW direction and associated with NE-SW, E-W, and N-S structures, characterize the brittle deformation. At Souwa, the large dolerite dykes, oriented NE-SW and NW-SE, fit into the post-Birimian NE-SW trending dyke system identified southeast of Téhini [28], and the area is marked by essentially brittle post-Eburnean deformation, comparable to the late deformation described in the Bliéron-Grand-Béréby sector [40] and the late NW-SE fractures that locally coincide with the direction of the dolerite dykes mapped at Tiébélé [38]. Metallogenically, gold mineralization is evidenced in the granodioritic plutonic unit, in a petrographic context close to many Birimian deposits (Tongon, Afema, Bonikro, Hiré, Bobosso, Angovia, Dougbafla...), where the presence or proximity of granitoid intrusions is systematic, even if these plutons are most often poorly mineralized, except for Bonikro [36], Hiré and Bobosso [35], as well as stockwork deposits developed in the granitoids of Ayanfuri and Julie in Ghana [37] [41]; at Souwa, the mineralization exhibits lithological control, with gold and sulfides disseminated in the granodiorite even in the absence of veins, but also a strong structural control, with the highest grades being associated with deformation intervals (shear zones, fractures, quartz veins and veinlets) which served as circulation pathways for mineralizing fluids, so that tectonics prepared the terranes both to host and preserve the mineralization; this distribution of gold, jointly controlled by lithology, structure, and hydrothermalism (fissure fillings of quartz and pervasive alterations of sericite, carbonates, hematite, sulfides, and silica), corresponds to a bimodal vein and disseminated mineralization, already described in most Birimian deposits of Côte d'Ivoire (Afema: [42]; Angovia and Tongon: [43]; Bonikro: [44]; Dougbafla: [45]) and more widely in West Africa [12].

6. Conclusion

The Souwa prospect is characterized by a granodioritic pluton crosscut by dolerite dykes, affected by regional greenschist facies metamorphism and thick meteoric alteration, superimposed on intense hydrothermal alteration, both pervasive and vein-type, marked by sericitization, carbonation, silicification, epidotization, chloritization, hematitization, and sulfidation, as well as quartz veins and veinlets, calcite, epidote, hematite, and ± sulfide veinlets. Deformations are of ductile-brittle type but dominated by brittle structures, organized into large NE-SW to NNE-SSW, NW-SE, and E-W sets, part of which corresponds to a post-Eburnean brittle phase, and which manifest as fractures, faults, veins, veinlets, shear zones, and dolerite dykes, genuine structural drains for mineralizing fluids. Gold mineralization, observed only in the host granodiorite, exhibits both lithological and structural control: on the one hand, gold (fine and associated with sulfides, mainly pyrite) is distributed in the granodiorite as disseminated mineralization and stockworks, even in the absence of well-developed veins; on the other hand, the richest drill intervals are systematically linked to more or less brecciated quartz lenses and veins, networks of veinlets and stockworks crosscutting fracture and shear zones, and associated with marked silicification, sericitization, carbonation, and sulfidation, confirming the hydrothermal affiliation of the mineralization and its tectonic control. This study contributes to the geological and metallogenic knowledge of the Souwa prospect and highlights the gold potential of the Birimian granitoid domains of the region; with a view to future work, it would be particularly useful (i) to conduct more detailed metallogenic studies to specify the ore paragenesis and the exact style of mineralization, (ii) to carry out a higher-resolution structural analysis based on radar images and geophysical data coupled with field observations to constrain the possible existence of a regional shear zone, and (iii) to deepen the petrographic study by electron microprobe thin section analyses to better characterize the mineralogy of the ores and the evolution of hydrothermal alterations.

Acknowledgements

This work was completed with the financial support of Ampella/Centamin Côte d'Ivoire and the Unit of Formation and Research of Earth Sciences and Mining Resources of Félix Houphouët-Boigny University (Abidjan-Cocody). The authors are grateful to the manager of Ampella/Centamin Pierrick Courderc, reviewers, and the editorial board staff.

Conflicts of Interest

The authors declare no conflicts of interest regarding the publication of this paper.

References

[1] Bessoles, B. (1977) Géologie de l'Afrique, Le craton ouest-africain. Les Mémoires du BRGM.

[2] Junner, N.R. (1940) Geology of the Gold Coast and Western Togoland. *Gold Coast Geological Survey Bulletin*, **11**, 75.

[3] Bates, D.A. (1956) Gold Coast and Togoland. Internat.4: Afrique No. 3: Afrique Occidentale Anglaise. In: *Lexique Stratigraphique International*, CNRS, 15-31.

[4] Milési, J.P., Ledru, P., Feybesse, J.L., Dommanget, A. and Marcoux, E. (1992) Early

Proterozoic Ore Deposits and Tectonics of the Birimian Orogenic Belt, West Africa. *Precambrian Research*, **58**, 305-344. https://doi.org/10.1016/0301-9268(92)90123-6

[5] Arnould, M. (1959) Étude stratigraphique et structurale des formations birimiennes de l'Afrique de l'Ouest. Service Géologique de Côte d'Ivoire.

[6] Tagini, B. (1971) Esquisse structurale de la Côte d'Ivoire: Essai de géotectonique régionale. Thèse de doctorat, Université Lausanne.

[7] Leube, A., Hirdes, W., Mauer, R. and Kesse, G.O. (1990) The Early Proterozoic Birimian Supergroup of Ghana and Some Aspects of Its Associated Gold Mineralization. *Precambrian Research*, **46**, 139-165. https://doi.org/10.1016/0301-9268(90)90070-7

[8] Feybesse, J.L., Billa, M., Guerrot, C., Duguey, E., Lescuyer, J.L., Milesi, J.P. and Bouchot, V. (2006) The Paleoproterozoic Ghanaian Province: Geodynamic Model and Ore Controls, Including Regional Stress Modeling. *Precambrian Research*, **149**, 149-196. https://doi.org/10.1016/j.precamres.2006.06.003

[9] Pouclet, A., Doumbia, S. and Vidal, M. (2006) Geodynamic Setting of the Birimian Volcanism in Central Ivory Coast (Western Africa) and Its Place in the Evolution of the Palaeoproterozoic of the Man Shield. *Bulletin de la Société Géologique de France*, **177**, 105-121. https://doi.org/10.2113/gssgfbull.177.2.105

[10] Jessell, M.W., Begg, G.C. and Miller, M.S. (2016) The Geophysical Signatures of the West African Craton. *Precambrian Research*, **274**, 3-24. https://doi.org/10.1016/j.precamres.2015.08.010

[11] Grenholm, M., Jessell, M. and Thébaud, N. (2019) A Geodynamic Model for the Paleoproterozoic (Ca. 2.27–1.96 Ga) Birimian Orogen of the Southern West African Craton—Insights into an Evolving Accretionary-Collisional Orogenic System. *Earth-Science Reviews*, **192**, 138-193. https://doi.org/10.1016/j.earscirev.2019.02.006

[12] Milési, J.P., Feybesse, J.L., Ledru, P., Dommanget, A. and Marcoux, E. (1989) Mineralizations of the West African Craton. *Journal of African Earth Sciences*, **9**, 147-171.

[13] Béziat, D., Dubois, M., Debat, P., Nikiéma, S., Salvi, S. and Tollon, F. (2008) Gold Metallogeny in the Birimian Craton of Burkina Faso (West Africa). *Journal of African Earth Sciences*, **50**, 215-233. https://doi.org/10.1016/j.jafrearsci.2007.09.017

[14] Hein, U.F., Klemd, R., Hirdes, W. and Nunoo, B.K. (2004) Structural Controls on Gold Mineralization in the Paleoproterozoic Birimian Terranes of Ghana. *Mineralium Deposita*, **39**, 361-376.

[15] Goldfarb, R.J., Groves, D.I. and Gardoll, S. (2001) Orogenic Gold and Geologic Time: A Global Synthesis. *Ore Geology Reviews*, **18**, 1-75. https://doi.org/10.1016/s0169-1368(01)00016-6

[16] Klemd, R. and Hirdes, W. (1997) Geochemical Constraints on the Genesis of Paleoproterozoic Lode Gold Mineralization in the Birimian of West Africa. *Mineralium Deposita*, **32**, 52-63.

[17] Perrouty, S., Agyei-Duodu, E. and Oberthür, T. (2015) Structural Evolution of the Paleoproterozoic Sefwi Gold Belt (Ghana). *Journal of African Earth Sciences*, **103**, 45-65.

[18] Kazapoe, R.W. (2023) Structural Controls and Mineralization Styles of Birimian Gold Deposits in West Africa. *Journal of African Earth Sciences*, **201**, Article 104795.

[19] Doumbia, S., Pouclet, A., Kouamelan, A., Peucat, J.J., Vidal, M. and Delor, C. (1998) Petrogenesis of Juvenile-Type Birimian (Paleoproterozoic) Granitoids in Central Côte-d'Ivoire, West Africa: Geochemistry and Geochronology. *Precambrian Research*, **87**, 33-63. https://doi.org/10.1016/s0301-9268(97)00201-5

[20] Kouadio, F.J.L.H., Kouamelan, A.N., Ouattara, A.S. and Djro, S.C. (2025) The Orthogneisses and Paragneisses of Sassandra-Cavally (SASCA) Domain (Côte d'Ivoire, West African Craton): Some Birimian Crustal Segments with a Strong Archaic Signature. *Journal of Geology and Mining Research*, **16**, 16-37. https://doi.org/10.5897/jgmr2025.0392

[21] Baratoux, L., Metelka, V., Naba, S., Jessel, M.W., Gregoire, M. and Ganne, J. (2011) Juvenile Paleoproterozoic Crust Evolution during the Eburnean Orogeny (~2.2-2.0 Ga), Western Burkina Faso. *Precambrian Research*, **191**, 18-45. https://doi.org/10.1016/j.precamres.2011.08.010

[22] Block, S., Ganne, J., Baratoux, L., Zeh, A., Parra-Avila, L.A., Jessell, M., *et al*. (2015) Petrological and Geochronological Constraints on Lower Crust Exhumation during Paleoproterozoic (Eburnean) Orogeny, NW Ghana, West African Craton. *Journal of Metamorphic Geology*, **33**, 463-494. https://doi.org/10.1111/jmg.12129

[23] Block, S., Jessell, M., Aillères, L., Baratoux, L., Bruguier, O., Zeh, A., *et al*. (2016) Lower Crust Exhumation during Paleoproterozoic (Eburnean) Orogeny, NW Ghana, West African Craton: Interplay of Coeval Contractional Deformation and Extensional Gravitational Collapse. *Precambrian Research*, **274**, 82-109. https://doi.org/10.1016/j.precamres.2015.10.014

[24] Arnould, M. (1961) Monographie des massifs de migmatiques et de granites Precambrien du nord-est de la Côte d'lvoire et de la Haute Volta méridionale. *Mémoires du BRGM*, **3**, 174.

[25] Lemoine, S. and Tempier, P. (1971) Sur le caractère orthogneissique des migmatites stratoides de ruines de Logbo. *Annales de l'Université d'Abidjan*, *Série C*, **7**, 65-80.

[26] Delor, C., Simeon, Y., Vidal, M., *et al*. (1995) Notice explicative de la carte géologique de la Côte d'Ivoire à 1/200 000, feuille de Nassian. Ministère des Mines et de l'Energie, DMG, Abidjan, Côte d'Ivoire, 32p.

[27] Vidal, M., Gumiaux, C., Cagnard, F., Pouclet, A., Ouattara, G. and Pichon, M. (2009) Evolution of a Paleoproterozoic "Weak Type" Orogeny in the West African Craton (Ivory Coast). *Tectonophysics*, **477**, 145-159. https://doi.org/10.1016/j.tecto.2009.02.010

[28] Lüdtke, G., Hirdes, W., Konan, G., Koné, Y., Yao, C., Diarra, S. and Zamble, Z. (1998) Géologie de la région Haute Comoé Nord avec carte géologique 1/100,000. Feuilles Kong. 4B, 4d, et Téhini-Bouna 3a-3d. Bulletin No. 1 DG Abidjan, 178p.

[29] Kone, P. (2015) Pétrologie des roches mafiques, ultramafiques et des granitoïdes associes aux ceintures de roches vertes de la région de Téhini (nord-est de la cote d'ivoire). Master's Thesis, Université Félix Houphouët-Boigny.

[30] Kouamé, K.M. (2015) Apport de l'imagerie géophysique aéroportée a la cartographie: Cas de Kalamon (nord-est de la côte d'ivoire). Ingenieur, STeRMI INPHB, 38p.

[31] Sonnendrucker, P. (1967) Etude de synthèse sur l'or en Côte d'Ivoire: La région aurifère du Sanwi. Société pour le développement minier de la Côte d'Ivoire (SODEMI), Abidjan, Rapport, 87p.

[32] Arnould, A. (1951) Rapport de mission géologique dans le Nord-est de la Côte d'Ivoire (feuille de Dabakala Est), Dir. Mines AOF, Dakar, 68p.

[33] Hirdes, W., Davis, D.W., Lüdtke, G. and Konan, G. (1996) Two Generations of Birimian Volcanic Belts in Northeastern Côte d'Ivoire (West Africa): Consequences for the 'Birimian Controversy'. *Precambrian Research*, **80**, 173-191. https://doi.org/10.1016/s0301-9268(96)00011-3

[34] Houssou, N.N. (2013) Etude pétrologique, structurale et métallogénique du gisement

aurifère d'Agbahou, Divo, Côte d'Ivoire. Doctorat Thesis, Université Félix Houphouët-Boigny.

[35] Gnanzou, A. (2014) Etude des series volcano-sédimentaires de la région de Dabakala (Nord-Est de la Côte d'Ivoire): Genèse et évolution magmatique. Contribution à la connaissance de la minéralisation aurifère de Bobosso dans la série de la Haute-Comoé. Doctorat Thesis, Université Félix Houphouët-Boigny.

[36] Ouattara, Z., Coulibaly, Y. and Lieben, F. (2015) Pétrographie du gisement d'or de Bonikro, sillon birimien d'Oumé—Fettékro, Côte d'Ivoire. *European Scientific Journal*, **11**, 132.

[37] Amponsah, P.O., Salvi, S., Béziat, D., Siebenaller, L., Baratoux, L. and Jessell, M.W. (2015) Geology and Geochemistry of the Shear-Hosted Julie Gold Deposit, NW Ghana. *Journal of African Earth Sciences*, **112**, 505-523. https://doi.org/10.1016/j.jafrearsci.2015.06.013

[38] Ilboudo, H., Lompo, M., Wenmenga, U., Naba, S., Kagambega, N. and Traore, S.A., (2008) Caractères pétrographiques et structuraux des formations paléoprotérozoïques (birimien) du gite a sulfures de Tiebele, burkina faso (Afrique de l'ouest). *Journal of Science*, **8**, 37-50.

[39] Hirst, T. (1942) The Geology of the Konongo Gold Belt and Surrounding Country. *The Gold Coast Geological Survey Bulletin*, **14**, 28.

[40] Kouadio, F.J.L.H. (2017) Étude pétro-structurale des formations géologiques du sud-ouest de la Côte d'Ivoire (secteur Bliéron-Grand Béréby): Apport de la géochimie et du couple déformation-métamorphisme. Doctorat Thesis, Université Félix Houphouët-Boigny.

[41] Yao, Y., Murphy, P.J. and Robb, L.J. (2001) Fluid Characteristics of Granitoid-Hosted Gold Deposits in the Birimian Terrane of Ghana: A Fluid Inclusion Microthermometric and Raman Spectroscopic Study. *Economic Geology*, **96**, 1611-1643. https://doi.org/10.2113/gsecongeo.96.7.1611

[42] Kadio, E., Coulibaly, Y., Allialy, M.E., Kouamelan, A.N. and Pothin, K.B.K. (2010) On the Occurrence of Gold Mineralizations in Southeastern Ivory Coast. *Journal of African Earth Sciences*, **57**, 423-430. https://doi.org/10.1016/j.jafrearsci.2009.11.008

[43] Coulibaly, Y., Boiron, M.C., Cathelineau, M. and Kouamelan, A.N. (2008) Fluid Immiscibility and Gold Deposition in the Birimian Quartz Veins of the Angovia Deposit (Yaouré, Ivory Coast). *Journal of African Earth Sciences*, **50**, 234-254. https://doi.org/10.1016/j.jafrearsci.2007.09.014

[44] Gnanzou, A. (2006) Etude lithostratigraphique de la région de Hiré dans le centre-sud de la Côte d'Ivoire (Permis de recherche PRA 37): Implication à la connaissance de la minéralisation aurifère. DEA, UFR-STRM, Université Félix Houphouët-Boigny.

[45] Sidik, O.A., Derving, B., Gbele, O. and Amadou, N. (2016) Mise En Evidence De Nouvelles Cibles De Forages A Partir De L'analyse De La Fracturation Du Prospect Aurifère de Dougbafla-OUME (Centre-Ouest De La Côte d'Ivoire). *European Scientific Journal*, **12**, 336-354. https://doi.org/10.19044/esj.2016.v12n36p336